

Lukas K. Tamm

Xing Han

Yinling Li

Alex L. Lai

Department of Molecular
Physiology and Biological
Physics,

University of Virginia,

Charlottesville,

VA 22908-0736

Structure and Function of Membrane Fusion Peptides

Abstract: Membrane fusion peptides are highly conserved hydrophobic domains of fusion proteins that insert into membranes during membrane fusion. Recent success with solving the structures of the influenza hemagglutinin fusion peptide and some critical mutants of this peptide in membrane environments at high resolution has led to a new understanding of the mechanism of membrane fusion. This review highlights the structures that have been solved and summarizes recent thermodynamic and spectroscopic studies on the interactions of this interesting class of peptides with lipid bilayers. © 2002 Wiley Periodicals, Inc. *Biopolymers (Pept Sci)* 66: 249–260, 2002

Keywords: membrane fusion; fusion peptide; host–guest peptide; NMR; CD; ATR-FTIR; spectroscopy; site-directed spin labeling; calorimetry

INTRODUCTION

Many cellular processes require two membranes to fuse into one. Examples are sperm–egg cell fusion, synaptic vesicle fusion at nerve termini, fusion of muscle cells into myoblasts, entry of enveloped viruses into cells, and intracellular vesicle traffic. In all these cases, membrane fusion is not a spontaneous process, but requires the action of highly specialized fusion proteins. Viral envelope proteins that mediate membrane fusion are among the best-studied fusion proteins. Influenza virus fusion, mediated by influenza hemagglutinin (HA), has been a particularly prominent model and has served as the paradigm for studying viral and nonviral membrane fusion mechanisms. Viral fusion proteins are in general large oligomeric structures that project far from the viral membrane

surface. Because of their appearance in electron micrographs and because they are usually glycosylated, they are often called spike glycoproteins. These spike glycoproteins undergo large conformational changes when triggered to perform the fusion reaction. In the case of influenza HA, the trigger is the mildly acidic pH (pH 5) that prevails in the endosomes of cells that have taken up the virus by endocytosis. The conformational changes of many other viral fusion proteins are triggered by binding to cell surface receptors. The conformational change exposes a highly conserved segment of the fusion protein, called the fusion peptide, which then becomes available for binding to and inserting into the lipid bilayer of the membranes to be fused. It is in general believed that the insertion of fusion peptides into membranes and the response of

Correspondence to: L. K. Tamm; email: lkt2e@virginia.edu
Biopolymers (Peptide Science), Vol. 66, 249–260 (2002)
© 2002 Wiley Periodicals, Inc.

Influenza Virus Fusion Peptide Sequences

<i>Description</i>	<i>Sequence</i>	<i>Activity</i>
	* * * * *	
Wild-type:	<u>GLFGAIAGFI</u> <u>ENGWEGMIDG</u> <u>WYGF</u> -	full fusion
G1S mutant:	<u>SLFGAIAGFI</u> <u>ENGWEGMIDG</u> <u>WYGF</u> -	hemi-fusion
G1V mutant:	<u>VLFGAIAGFI</u> <u>ENGWEGMIDG</u> <u>WYGF</u> -	no fusion
 <i>Host-Guest Fusion Peptide Models</i>		
P8H7	GLFGAIAG -GCGKKKK	0.07 % / min
P13H7	GLFGAIAGFIENG -GCGKKKK	0.5 % / min
P16H7	GLFGAIAGFIENGWEG -GCGKKKK	2.5 % / min
P20H7	GLFGAIAGFIENGWEGMIDG -GCGKKKK	5.3 % / min
G1S-P20H7	SLFGAIAGFIENGWEGMIDG -GCGKKKK	n.d.
G1V-P20H7	VLFGAIAGFIENGWEGMIDG -GCGKKKK	n.d.

FIGURE 1 Sequences of influenza hemagglutinin fusion peptides. (Top) The first 24 residues of strain X:31 (A/Hongkong/68) HA2 are shown. The residues shown in boldface are highly conserved between all influenza strains. Large apolar residues (underlined) and glycines (asterisks) occur in heptad repeat patterns. Two critical mutations of the first residue are also shown. (Bottom) Sequences of host-guest fusion peptides used in our studies. The fusion peptide (guest) portions are shown in boldface and the polar host portions in normal face. The fusion activities are measured by a fluorescent lipid mixing assay (from Ref. 10). n.d., not determined.

membranes to their insertion are the central events that lead to membrane fusion. In this review, we summarize what can be gleaned from studies of model fusion peptides and their interactions with model membranes and how the results obtained from such model studies might relate to cellular membrane fusion reactions. Although we focus entirely on fusion peptides from influenza HA and HA-mediated membrane fusion, it is likely that the fusion reaction mediated by other viral and even nonviral fusion proteins are variations of the general theme that has emerged from studies of influenza HA membrane fusion.

MEMBRANE FUSION PEPTIDES

Fusion peptides are sequences of 20 to 30 mostly, but not exclusively, apolar residues of the fusion-promoting subunits of fusion proteins. The sequences of fusion peptides are highly conserved within each family of viruses, but less conserved across different virus families. In many viral fusion proteins, the fusion peptides reside at the extreme N-terminus of the fusion-promoting subunit. However, a few viral fusion proteins harbor internal fusion peptides that are em-

bedded within the sequence of the fusion-promoting subunit. Fusion peptides are in general rich in alanines and glycines. For example, the fusion peptide of the fusion protein gp41 of the human immunodeficiency virus contains 20% glycyl and 23% alanyl residues. The glycine and alanine contents of influenza HA are 29 and 8%, respectively. These unusual amino acid compositions immediately suggest that fusion peptides may be conformationally flexible and may adapt their structures depending on the environment. Conformational properties of fusion peptides and possible functional implications of their conformational plasticity have been discussed in more detail elsewhere.¹

Figure 1 shows the consensus sequence of the fusion peptide of strain A influenza HA. Most residues in the N-terminal half of the sequence are highly conserved (shown in boldface). Bulky hydrophobic side-chains (underlined) and glycines (asterisks) are arranged in phase-shifted heptad repeat patterns (four and three residues apart) that would place these residues on opposite faces if the peptide folded into a regular α -helix. An amphipathic helix could thus be formed with a highly hydrophobic bulky face and a more hydrophilic glycine-rich face. The regularity of

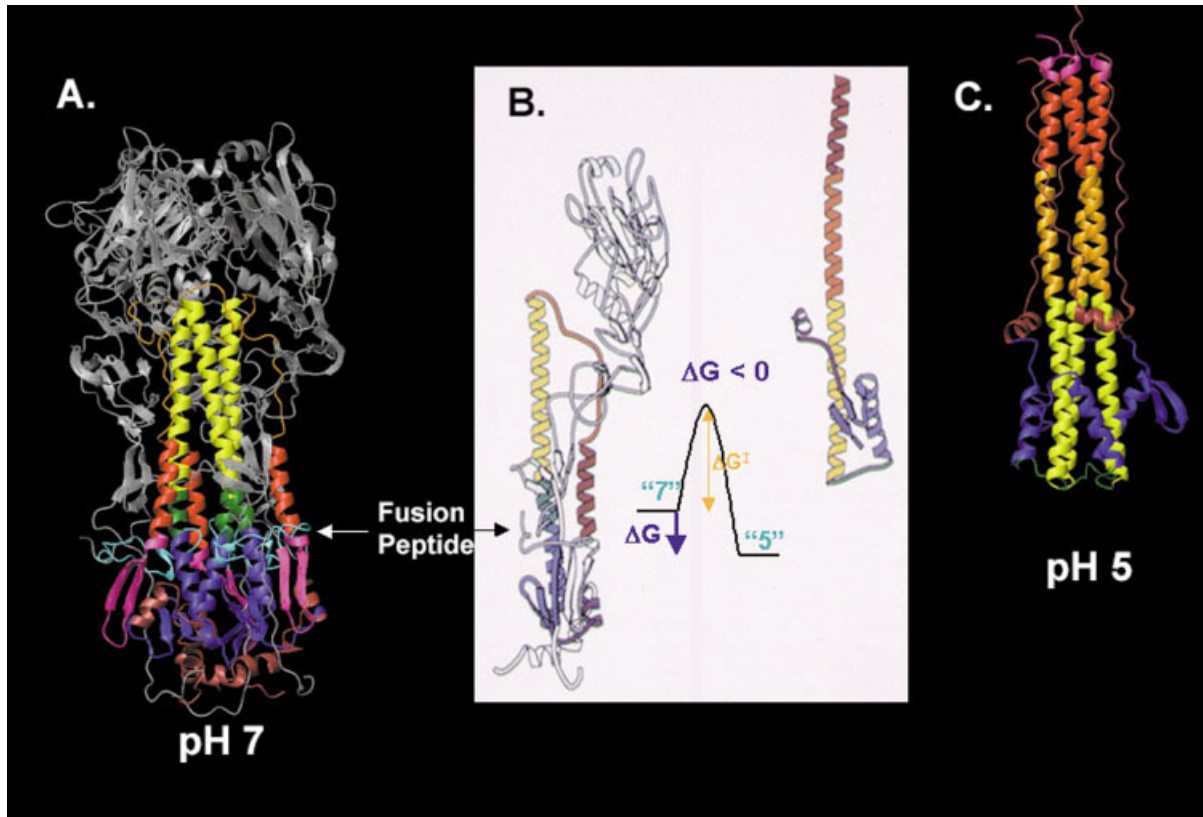


FIGURE 2 Structures and refolding of influenza hemagglutinin. (A) Crystal structure of the bromealin-cleaved ectodomain of strain X:31 influenza HA at pH 7 (from Ref. 5). The three HA1 chains are shown in grey. The three HA2 chains are shown in colors. The fusion peptides are highlighted in cyan. The cleaved transmembrane domain that anchors the protein in the viral membrane would be attached to the brown chain at the bottom of the shown structure. (B) Cut-out diagram of one monomer of the trimeric crystal structures showing the low pH-induced refolding of the HA2 chain. Corresponding polypeptide regions are highlighted in the same colors. The energy diagram indicates the gain in free energy upon refolding. (C) Crystal structure of the bromealin- and thermolysin-cleaved HA2 core of strain X:31 influenza HA at pH 5 (from Ref. 7). The HA1 chains are not present in this structure. The fusion and transmembrane peptides would be located at the top of this structure attached to the pink N- and brown C-termini, respectively.

this general pattern appears to be broken around residues 11 and 12, i.e., about in the middle of this fusion peptide sequence. Many single-site mutations in the fusion peptide abolish or alter the fusion phenotype of the whole protein.^{2–4} Effects of mutating the first residue have been studied in most detail. For example, if this residue is changed from a glycine to a serine cells expressing full-length HA fuse their membranes with those of target cells, but a fully grown fusion pore that allows exchange of cytoplasmic contents is not promoted by this mutant.⁴ This phenotype, which is characterized by lipid mixing but not contents mixing, is called hemifusion. The hemifused state is thought to be an intermediate state on the fusion reaction pathway. If glycine 1 is changed to a valine, neither hemifusion

nor full fusion is observed. This mutation completely blocks fusion.⁴

STRUCTURES OF THE ECTODOMAIN OF INFLUENZA HEMAGGLUTININ

Two structures of the soluble portion, i.e., the ectodomain of influenza hemagglutinin have been solved by X-ray crystallography.^{5–7} Figure 2 shows an overview of these structures and how they are conformationally related to each other. HA is a trimer at both the resting pH 7 [Figure 2(A)] and the fusion pH 5 [Figure 2(C)]. Each monomer in the trimer consists of two polypeptide chains, HA1 and HA2. HA1 is shown in white and HA2 in various colors in Figure 2(A). HA2 also

contains the transmembrane domain, which anchors HA in the viral membrane that would be located at the bottom of the shown structure. The transmembrane domain and a short intraviral C-terminal segment of HA2 have been proteolytically removed from this fragment of HA to obtain crystals that were suitable for the X-ray diffraction. A prominent feature of the structure are the long α -helical coiled coils formed by HA2 (shown in yellow-green-blue). The fusion peptides at the N-termini of HA2 are shown in cyan. Upon activation by pH 5, HA2 undergoes massive refolding [Figure 2(B)]. The fusion peptide is extruded from a hydrophobic protective crevice in the pH 7 structure. A loop shown in orange becomes helical at pH 5 and extends the coiled coil. The lower part of the original coiled coil (shown in blue) breaks off and folds antiparallel to the coiled coil at pH 5. These events move the fusion peptide, which was proteolytically removed from the fragment that was crystallized, to the top of the molecule, i.e., toward where the target membrane would be bound. The fragment that was crystallized at pH 5 not only lacks the transmembrane domain and the fusion peptide, but also the entire HA1 chain.

Several studies have shown that the pH 5 structure is at a lower free energy than the pH 7 structure. Therefore, energy must be released during refolding from the pH 7 to the pH 5 structure.⁸ This energy likely contributes to driving membrane fusion, which by itself is an energetically unfavorable process.

The crystal structures of the HA fragments have provided an excellent framework for conceiving structure-based mechanisms by which membrane fusion may proceed. However, because all membrane-interactive domains have been removed from these molecules, their use for obtaining further structural insight into the mechanism of membrane fusion is limited. The structures of the membrane-interactive parts, namely those of the transmembrane domains and the fusion peptides, also need to be solved in membrane environments to understand how fusion works at the molecular structural level.

FUSION PEPTIDES LIKELY FORM INDEPENDENTLY FOLDED DOMAINS IN MEMBRANES

The sequence that leads from the C-terminal end of the fusion peptide to the soluble fragment that has been solved by X-ray crystallography at pH 5 is likely disordered. This region includes residues 25–33 of HA2. The sequence of this region, which is contiguous with the fusion peptide sequence shown in Figure

1, is Arg-His-Gln-Asn-Ser-Glu-Gly-Thr-Gly. Although these residues were present in the expressed construct that was used in the most recently refined crystallographic structure of low pH HA2, they were disordered.⁷ The crystallographically ordered structure begins at residue 34 of HA2 with an extended, but strongly hydrogen-bonded N-cap that leads into the triple coiled coil beginning at residue 38. The intervening sequence shown above is polar and therefore not expected to interact with membranes. This sequence is also readily accessible to digestion by thermolysin or trypsin in low pH-treated HA2.⁹ As will be discussed below, the fusion peptide forms well-defined structures in membranes at neutral and low pH. Given these structural and biochemical results, it is likely that the ectodomain and fusion peptide of HA2 form two separately folded domains linked by a flexible linker comprising residues 25–33. Therefore, we sometimes call the fusion peptide also the “fusion domain” of HA2.

STRATEGY: HOST-GUEST FUSION PEPTIDES

A problem that has plagued the fusion peptide field for many years is their relatively low solubility in polar and apolar solvents. Most full-length fusion peptides are too hydrophobic to be soluble in water. On the other hand, they also contain a significant number of polar residues, which make them difficult to dissolve in many apolar solvents as well. Solvents that have in general worked well for fusion peptides are dimethyl-sulfoxide and hexafluoro-isopropanol. Even if fusion peptides are soluble in these solvents, they are not easily recombined with lipid bilayer model membranes from these solvents. It is well known that the structure and behavior of apolar peptides in lipid bilayers can depend dramatically on sample preparation techniques and therefore on the solvent history. Gramicidin A, for example, adopts different structures in membranes, depending on the solvent from which and how it was recombined with membrane lipids. Therefore, it is not surprising that many different, often dramatically conflicting results have been reported about structures and interactions of fusion peptides with lipid bilayers.

In physiological fusion reactions, the fusion peptides are delivered from the crevice of the pH 7 structure of HA to the target membrane in an aqueous environment. To mimic this process as closely as possible, we designed a new generation of fusion peptides, which we call “host-guest” fusion peptides.¹⁰ In this approach the “guest” fusion peptides

Table I Energies of Interaction of Influenza Hemagglutinin Fusion Peptides with Lipid Bilayers

Peptide	$\Delta\Delta G^a$ (kcal/mol)	$\Delta\Delta H^b$ (kcal/mol)	$T\Delta\Delta S$ (kcal/mol)	$\Delta\Delta S$ (cal/mol · K)
P8	-0.2	-4.2	4.0	-13.3
P13	-2.7	-9.5	6.8	-35.5
P16	-5.1	-16.3	11.2	-37.6
P20	-7.6	-18.0	10.4	-34.8
G1S-P20	-6.9	-15.9	9.0	-30.3
G1V-P20	-5.5	-9.2	3.7	-13.3

^a From Ref. 10.^b Y. Li and L. K. Tamm, unpublished results.

are linked at their C-terminus to a polar carrier “host” peptide that renders the entire construct water soluble. The host peptide therefore replaces in a sense the entire polar ectodomain of HA. The linker between the guest and host portions of these peptides is designed to be conformationally flexible to prevent distortion of the structure and interactions of the fusion peptide with lipid model membranes. Therefore, host-guest fusion peptides likely preserve the native, physiological fusion domain structure. The actual designs of some host-guest fusion peptides of different lengths are shown in the lower part of Figure 1. Because they contain different lengths starting from the N-terminus of the HA fusion peptide sequence, these peptides could also mimic the development of the fusion peptide structure as it “grows” into a model target membrane. The host-guest fusion peptides shown in Figure 1 are all highly soluble in aqueous buffers of low ionic strength. They also bind readily to target lipid model membranes. A small fraction of negatively charged lipids, as often found in real biologic membranes, promote their binding. Increasing the length of the host-guest fusion peptides increases their fusion activities as measured by a lipid mixing fusion assay.

ENERGETICS OF MEMBRANE INTERACTIONS

The high solubility of the host-guest fusion peptides permits detailed thermodynamic binding studies to be performed with lipid model membranes. We studied the binding of the influenza HA fusion peptides to lipid bilayers by fluorescence spectroscopy and isothermal titration calorimetry (ITC). The binding data obtained by the fluorescence enhancement of the NBD reporter group in the apolar environment of lipid bilayers are best analyzed by a partition equilibrium.

The measured partition coefficient, K , is then converted into the free energy of binding, ΔG , using the familiar relation $\Delta G = -RT\ln K$. The same measurement is also carried out with the host peptide alone. To obtain the free energies of binding for the fusion peptide portions of the host-guest peptides, we calculate $\Delta\Delta G = \Delta G$ (host-guest) - ΔG (host). The resulting values for the peptides shown in Figure 1 are shown in Table I. Not surprisingly, the longer the fusion peptide, the more negative free energies of binding are observed, indicating increased hydrophobic interactions of the longer fusion peptides with the lipid bilayer.

A more detailed analysis of the interaction involves the separate determination of enthalpic and entropic contributions to the binding free energy. Enthalpies of binding, ΔH , are measured by ITC and corrected for contributions from the host peptide in the same way as described above for ΔG . Knowing $\Delta\Delta G$ and $\Delta\Delta H$ then immediately yields $\Delta\Delta S$, the entropy of binding, by $\Delta\Delta G = \Delta\Delta H - T\Delta\Delta S$. The values of $\Delta\Delta H$ and $\Delta\Delta S$ are also listed in Table I. The most striking result of the data of Table I is that the binding of fusion peptides to lipid bilayers is not entropically but rather enthalpically driven. This is in contradiction to the common notion that insertion of these peptides is driven by the “classic” hydrophobic effect, which is a process that is dominated by the gain in water entropy.¹¹ Rather, fusion peptide insertion is dominated by a gain in enthalpy, i.e., a “non-classic” hydrophobic effect.¹²

STRUCTURES OF FUSION PEPTIDES IN MEMBRANES

Early circular dichroism (CD) and Fourier transform infrared (FTIR) studies of the influenza HA fusion peptide indicated that this peptide is 40–60% α -heli-

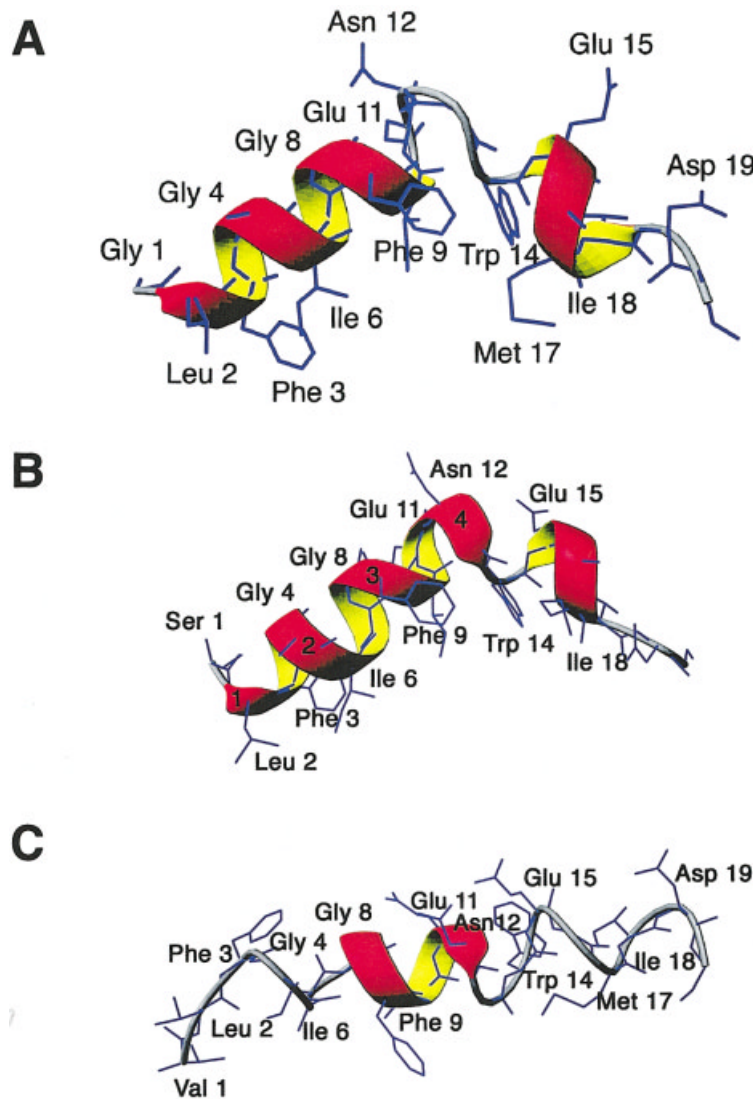


FIGURE 3 NMR structures of wild-type and mutant influenza hemagglutinin fusion peptides in dodecyl-phosphocholine micelles in pH 5 buffer. (A) The wild-type structure is characterized by an N-terminal α -helix, a bend at Asn12, and a C-terminal 3_{10} -helix. The angled (boomerang-shaped) structure encloses a hydrophobic pocket between the two arms. Gly1, Gly4, and Gly8 form a glycine edge on the outer rim of the N-terminal helix (from Ref. 24). (B) The G1S mutant structure differs from the wild-type structure by a disrupted glycine edge and a more irregular N-terminal helix. (C) The G1V mutant structure is characterized by an irregular linear amphipathic helix. (B and C: X. Han, J. H. Bushweller, and L. K. Tamm, unpublished results.)

cal in lipid model membranes.^{13–18} Some of these studies also indicated small fractions of β -structure in these peptides. As mentioned above, the relative contents of helix and extended structures depended on the length of the peptide models and the methods of model membrane preparation. Polarized attenuated total reflection (ATR) FTIR also allows one to determine the order parameter of the helical segment in the lipid bilayer.¹⁹ The order parameter is a measure of

the orientational distribution of the peptide in the bilayer and is defined as $S = \frac{1}{2} \langle 3 \cos^2 \theta - 1 \rangle$, where θ is the angle of the peptide axis (e.g., the α -helix) to the bilayer normal and the angular brackets denote how the distributions are averaged. The α -helical segment(s) of the influenza HA fusion peptide were found to be inserted at oblique angles, ranging from about 20 to 60°, in these measurements.^{17,18,20–22} Again, the different results obtained in different lab-

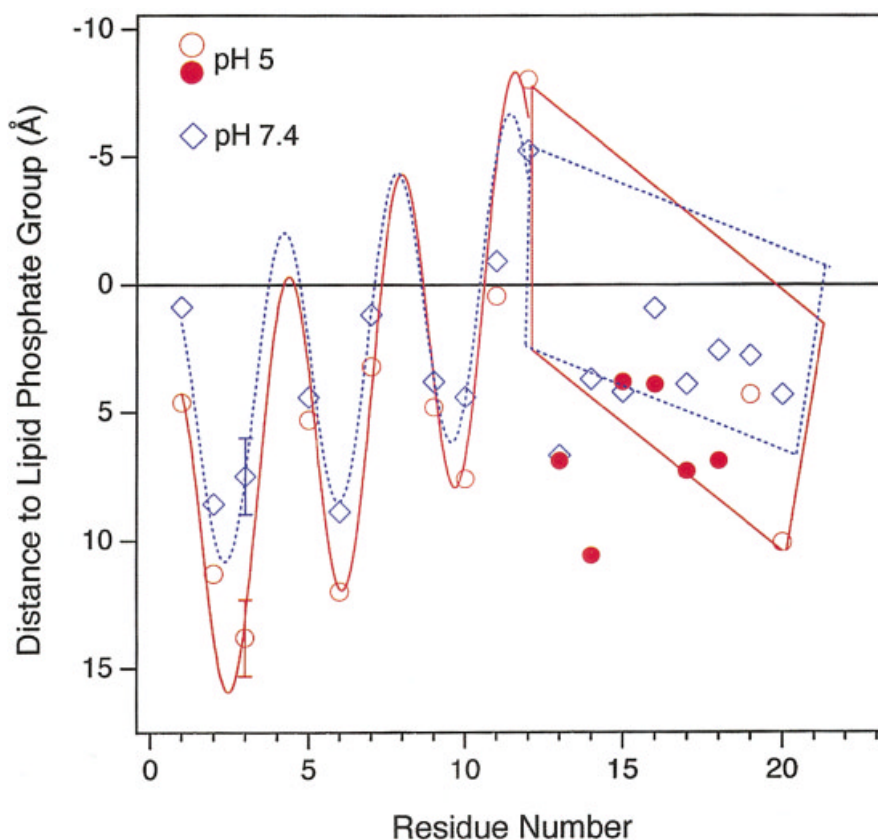


FIGURE 4 Topology of influenza hemagglutinin fusion peptide in lipid bilayers at pH 7.4 (blue) and pH 5 (red). The depths of membrane insertion were measured by power-saturation EPR spectroscopy of site-directed spin-labeled fusion peptides. The angled structure determined in lipid bilayers is consistent with an N-terminal helix, a bend at Asn12, and a C-terminal helical turn (at pH 5) and is highly reminiscent of the NMR structure determined in detergent micelles and presented in FIGURE 3 (A) (from Ref. 24).

oratories most likely reflect the different sample preparation methods that were employed in these laboratories. Other differences can be accounted for by different parameters that have been used in the analytic expressions to extract the order parameter from the measured dichroic ratios. The new host-guest fusion peptides resolved some of these issues because peptide aggregation in solution and in membranes can be controlled.²³ Monomeric P20H7 is about 90% random coil in solution and adopts about 48% α -helical secondary structure in detergent micelles or lipid bilayers.¹⁰ The average orientation of the α -helical segments from the membrane surface is about 33° .¹⁰

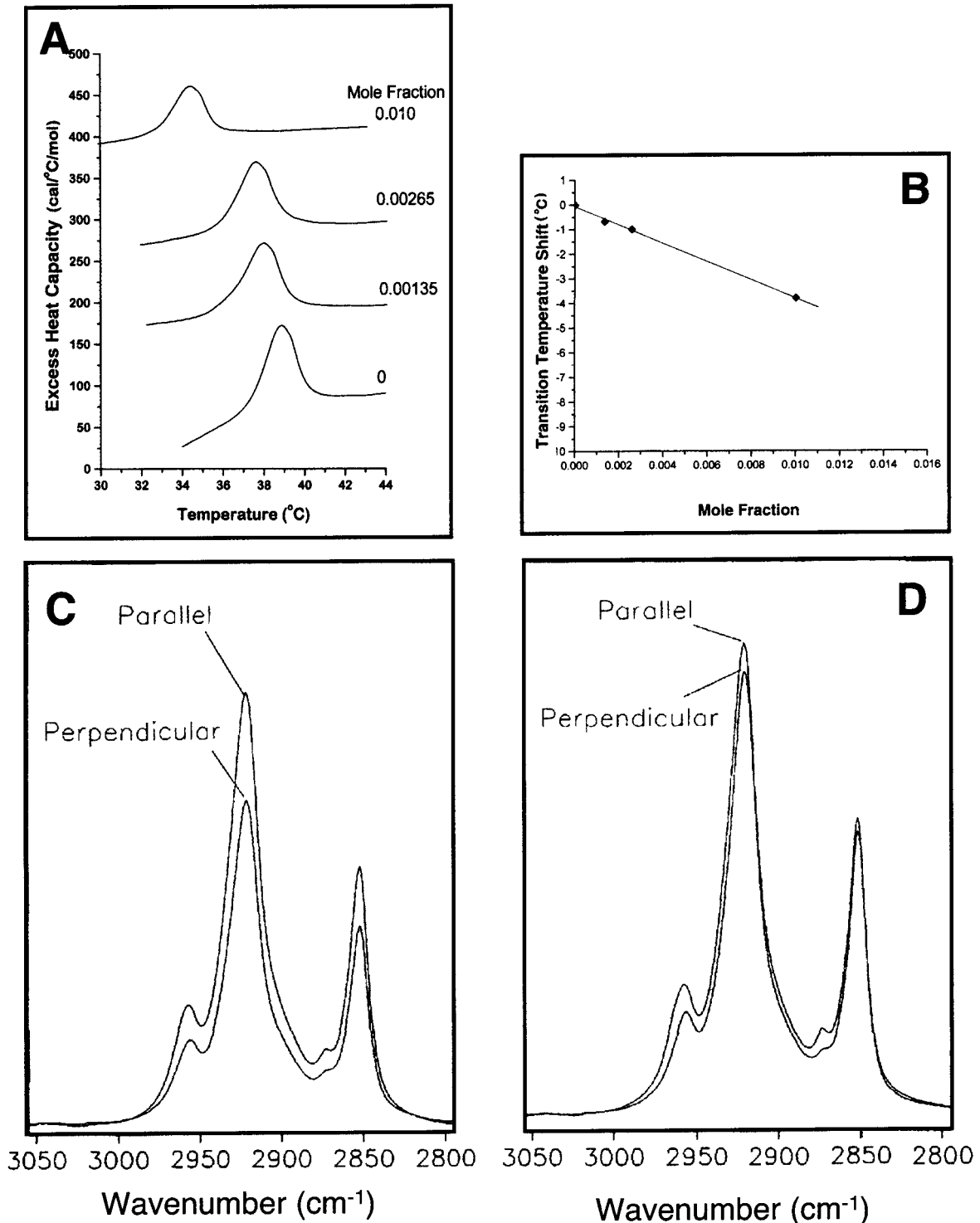
Recently, we determined the atomic resolution structure of P20H7 in detergent micelles and lipid bilayers by nuclear magnetic resonance (NMR) and site-directed spin-label electron paramagnetic resonance (EPR) spectroscopy.²⁴ This is the first high-resolution structure of any membrane fusion peptide that has been solved in a membrane environment. The

NMR structure determined in dodecyl-phosphocholine micelles is shown in Figure 3(A). Surprisingly, the structure does not consist of a single helix, but rather two helices interrupted by a kink around Asn12, i.e., the position where the heptad repeat was interrupted (see Figure 1). The overall structure is therefore characterized by an angled V or boomerang shape with all bulky apolar residues pointing toward a hydrophobic pocket in the center of the V. The conserved glycines form a glycine edge on the outer surface of the N-terminal arm of the fusion peptide. The C-terminal arm consists of a single turn of 3_{10} -helix and some residues in irregular conformations. The C-terminal arm is less ordered than the N-terminal arm, which is also more conserved in sequence across different viral strains. The angle between the two arms is about 105° and is stabilized by several hydrogen bonds in the kink region.

The structure determined by NMR in detergent micelles is preserved in lipid bilayers as shown by

spin-label EPR spectroscopy (Figure 4). In these experiments, each of the 20 residues of the fusion peptide was individually changed into a cysteine and then labeled with the spin label (1-oxy-2,2,5,5-tetramethyl- Δ^3 -pyrroline-3-methyl) methanethiosulfonate. Power sat-

uration of the spin-label EPR spectra in the presence of nitrogen, oxygen, and nickel(II)-ethylenediamine-*N,N'*-diacetic acid yields a precise ($\pm 2 \text{ \AA}$) measure of the depth of the unpaired electron of the spin label in the membrane.²⁵ Figure 4 shows these depths mea-



sured as distances from the average position of the phosphorus atoms of the phospholipids in the bilayer. The boomerang structure with an N-terminal helical arm and a single helical turn in the C-terminal arm at pH 5 is well reproduced in this structure. We therefore conclude that the structure of the fusion peptide in lipid bilayers is essentially the same as in detergent micelles and that the vertex of the boomerang, i.e., the α -carbon of Asn12, is positioned at the same level as the phosphate groups in the lipid bilayer.²⁴ The peptide penetrates the bilayer to about 15 Å from the phosphates, i.e., it reaches almost, but not quite, to the center of the lipid bilayer. The angle of the N-terminal arm with the membrane surface is about 38°, i.e., close to the 33° that have been estimated before for the average of both arms by polarized ATR-FTIR spectroscopy.

We also solved by NMR the structures of the hemifusion mutant G1S and the fusion-blocking mutant G1V in dodecyl-phosphocholine micelles [Figures 3(B) and 3(C)]. The overall shape of the G1S mutant is similar to that of the wild-type peptide. It also forms the boomerang, but the N-terminal tip of the boomerang and the glycine edge are disrupted by a hydrogen bond that is formed from the Ser1 side-chain to the amide hydrogen of Gly4. The G1V mutant peptide forms a linear irregular helical structure. The boomerang shape is no longer evident in this mutant. The reason for this dramatically altered structure of the nonfusogenic mutant is that the Val1 side-chain is rotated toward the hydrophobic core of the micelle whereas Phe3 is pushed toward the micelle surface compared to the wild-type structure. The different interactions with the interface apparently propagate as far as into the kink region, where they abolish the hydrogen bonds that define the kink of the wild-type and G1S structures. Interestingly, the hydrophobic interaction energies of the G1S and G1V mutants with lipid bilayers are also reduced to -6.9 kcal/mol and -5.5 kcal/mol, respectively, compared to -7.6 kcal/mol for the wild-type peptide (Table I).

Reduced hydrophobic interactions would be expected for peptides that do not penetrate as deeply as the wild-type peptide. The CD spectra of these peptides in detergent micelles and lipid bilayers are virtually identical, indicating that the structures of these peptides in lipid bilayers may be the same as in dodecyl-phosphocholine micelles.

FUSION PEPTIDES ALTER THE STRUCTURE OF LIPID BILAYERS

Fusion peptides exert a variety of effects on the bilayer structure of membranes that are not all fully understood yet. One effect that has been seen with fusion peptides from several viruses is their ability to alter the phase behavior of lipids that are prone to form hexagonal phases at elevated temperatures. One such lipid is dipalmitoleoyl-phosphatidylethanolamine (DiPoPE). This lipid forms normal bilayers in the liquid-crystalline (L_{α}) phase below 42° C. Above this temperature, DiPoPE forms highly curved hexagonally packed tubes with the polar headgroups pointing toward the center of the tube. This phase is called the H_{II} phase. The $L_{\alpha} \rightarrow H_{II}$ phase transition temperature, T_H , decreases when fusion peptides are added at increasing concentrations to DiPoPE bilayers [Figure 5(A)]. This effect has been attributed to the ability of the fusion peptide to decrease the intrinsic negative curvature of these lipid bilayers to the extent that they are no longer stable, but change into the more highly negatively curved H_{II} phase.²⁶ Bending of bilayers is thought to be necessary to form intermediates in membranes fusion.^{27,28}

Another prominent effect of fusion peptides on the structure of lipid bilayers has been determined by observing changes of the dichroic ratio of polarized ATR-FTIR bands of the lipid methylene chains upon insertion of fusion peptides into membranes. An example is shown in Figure 5(B). The two main peaks in these spectra arise from the antisymmetrical and sym-

FIGURE 5 Interactions of the influenza hemagglutinin fusion peptide with membrane lipids. The experiments of this figure were carried out with the wild-type fusion peptide sequence (first 23 residues) without the polar host peptide. (A) Differential scanning calorimetry traces showing the lamellar-to-hexagonal phase transition of DiPoPE in peptide-lipid complexes with increasing mole fractions of peptide. (B) Shift of the lamellar-to-hexagonal transition temperatures derived from (A) as a function of fusion peptide concentration in the lipid bilayer. The slope of the straight line is -380° C mole lipid/mole peptide. (C) Methylene stretching region of polarized ATR-FTIR spectra of a single supported dimyristoyl-phosphatidylcholine bilayer in pH 5 buffer. The acyl chain order parameter derived from the dichroic ratio (= parallel/perpendicular absorption) is 0.4. (D) Same as in (C) but with 10 mole % fusion peptide included. The acyl chain order parameter derived from the dichroic ratio is 0.7, i.e., the lipid chains are more ordered in the presence than in the absence of the fusion peptide. (A and B: R. Epanand L. K. Tamm, unpublished results; C and D: from Ref. 17.)

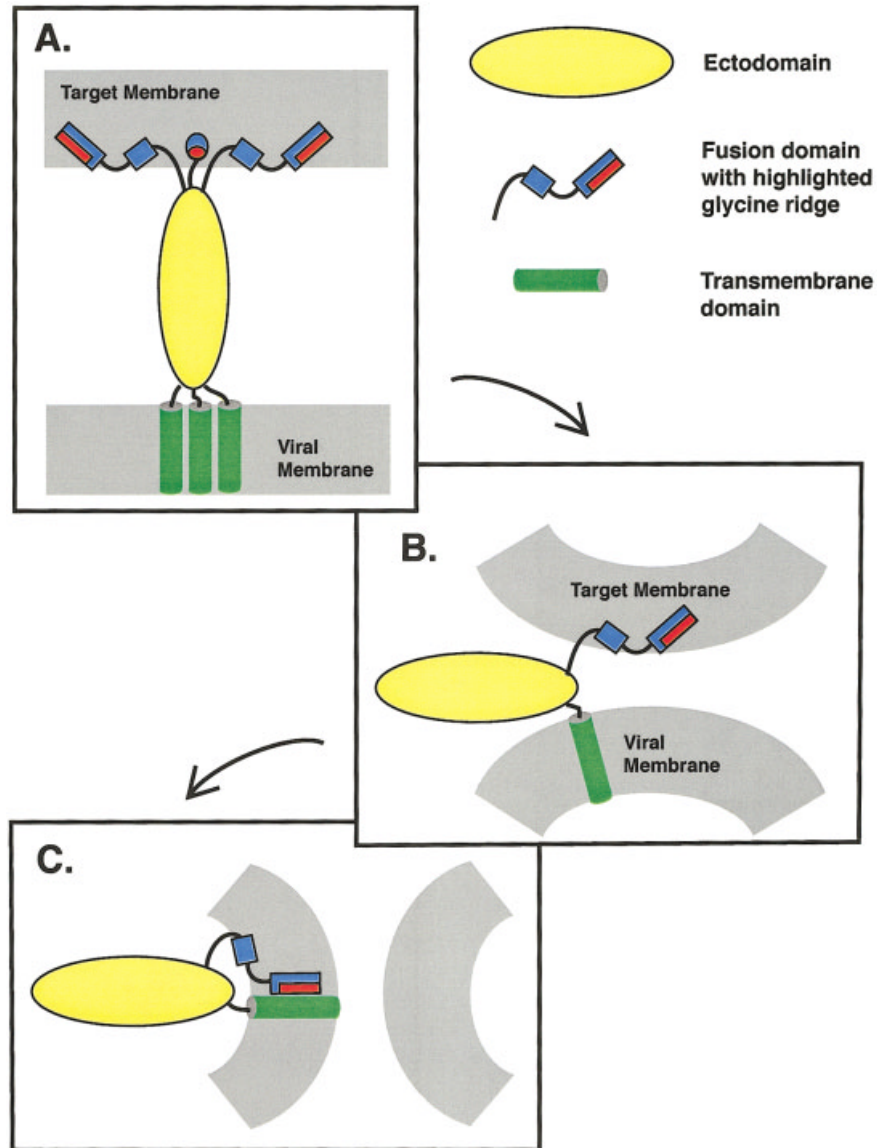


FIGURE 6 Boomerang model of influenza hemagglutinin-mediated membrane fusion. (A) The pH-induced conformational change in the ectodomain thrusts the boomerang-shaped fusion peptides toward the target membrane where it inserts. (B) The ectodomain tilts relative to the two membrane planes. The boomerang retrieves the target membrane and brings it to close juxtaposition with the viral membrane such that lipid exchange (hemifusion) can occur. (C) The fusion peptide and transmembrane domain are thought to interact by virtue of the glycine-edge of the fusion peptide to open the initial fusion pore.

metrical CH_2 stretching vibrations of the acyl chains of dimyristoyl-phosphatidylcholine. In pure lipid bilayers, the ratio of the absorbance of parallel polarized light to the absorbance of perpendicular polarized light is about 1.3. In the presence of 10 mole % of peptide, this ratio decreases to 1.05. Using the pertinent analytic expressions, one calculates a change of the lipid acyl chain order parameter, S , from 0.4 in the absence to 0.7 in the presence of the fusion peptide.

The acyl chains become more ordered in the presence of the fusion peptide. Increased lipid ordering may be correlated with a partial dehydration of the lipid headgroups.²⁹ Direct evidence for alterations of the hydration layer and hydrogen bonding interactions at the lipid-water interface was also obtained from ATR-FTIR spectroscopy.¹⁷ The region around 1735 cm^{-1} reports on the state of hydrogen bonding of the lipid ester carbonyl groups.¹⁹ In pure lipid bilayers, a single

broad band composed of two poorly resolved bands is observed at 1735 cm^{-1} , but in the presence of increasing amounts of the influenza HA fusion peptide the two component bands move further apart and become increasingly better resolved. Dehydration at the membrane surface may be a prerequisite for membrane fusion.

LINKING INSIGHTS FROM STUDIES OF FUSION PEPTIDES TO THE PHYSIOLOGICAL PROCESS OF MEMBRANE FUSION

How do these results obtained with fusion peptides relate to the physiological process of membrane fusion? We propose a “boomerang model” for HA-mediated membrane fusion as depicted in Figure 6. In this model, we envisage the following steps: (1) The pH-induced conformational change of HA extrudes the fusion peptide from the hydrophobic crevice shown in Figure 2(A). (2) It also extends the coiled coil toward the target membrane as shown in Figure 2(B). (3) This allows the fusion peptide to insert into the target membrane where it adopts the boomerang structure shown in Figure 3(A) and schematically depicted in Figure 6(A). All these steps are exothermic. Energy is gained by forming the extended coiled coil of the low-pH structure,⁸ by forming the N-cap at the end of the triple coiled coil at pH 5⁷ and by the insertion of the fusion peptide into the lipid bilayer of the target membrane (Table I). This energy can be expended on dehydrating and possibly bending the membranes to be fused. (4) Polarized ATR-FTIR experiments have shown that the triple coiled coils of the ectodomain tilt toward the plane of the viral and target membranes.^{30,31} This lateral excursion of the ectodomain will pull the two membranes close to each other, i.e., the boomerang will be retrieved toward the target membrane as shown in Figure 6(B). (5) Dehydration and possibly other perturbations of the target and viral membrane³² will further decrease the distance between the two membranes to the extent that the lipids of the two proximal leaflets begin to mix. This is the hemifused state. The structure of this intermediate is not well known. Therefore, we do not attempt to draw a picture of this intermediate. (6) Because the boomerang shape with an intact glycine edge of the fusion peptide and a fully extended transmembrane domain³³ are both required to progress to a full fusion pore and because the C- and N-terminal ends of the ectodomain are in close proximity to each other,⁷ it is tempting to speculate that a direct interaction between the fusion peptide and the transmem-

brane domain may be required to open the fusion pore. This is shown in Figure 6(C). Although such an interaction has not yet been demonstrated in the influenza or in any other fusion system, there are precedents in the literature for helix-helix interactions that are mediated by glycine-rich helical surfaces.³⁴

This work was supported by NIH grant AI 30557.

REFERENCES

1. Tamm, L. K.; Han, X. *Biosci Reports* 2000, 6, 501–518.
2. Gething, M. J.; Doms, R. W.; York, D.; White, J. *J Cell Biol* 1986, 102, 11–23.
3. Steinhauer, D. A.; Wharton, S. A.; Skehel, J. J.; Wiley, D. C. *J Virol* 1995, 69, 6643–6651.
4. Qiao, H.; Armstrong, R. T.; Melikyan, G. B.; Cohen, F. S.; White, J. M. *Mol Biol Cell* 1999, 10, 2759–2769.
5. Wilson, I. A.; Skehel, J. J.; Wiley, D. C. *Nature* 1981, 289, 366–373.
6. Bullough, P. A.; Hughson, F. M.; Skehel, J. J.; Wiley, D. C. *Nature* 1994, 371, 37–43.
7. Chen, J.; Skehel, J. J.; Wiley, D. C. *Proc Natl Acad Sci USA* 1999, 96, 8967–8972.
8. Carr, C. M.; Kim, P. S. *Cell* 1993, 73, 823–832.
9. Ruigrok, R. W. H.; Aitken, A.; Calder, L. J.; Martin, S. R.; Skehel, J. J.; Wharton, S. A.; Weis, W.; Wiley, D. C. *J Gen Virol* 1988, 69, 2785–2795.
10. Han, X.; Tamm, L. K. *Proc Natl Acad Sci USA* 2000, 97, 13097–13102.
11. Tanford, C. H. *The Hydrophobic Effect: Formation of Micelles and Biological Membranes*; Wiley: New York, 1980.
12. Seelig, J.; Ganz, P. *Biochemistry* 1991, 30, 9354–9359.
13. Murata, M.; Sugahara, Y.; Takahashi, S.; Ohnishi, S.-I. *J Biochem* 1987, 102, 957–962.
14. Lear, J. D.; DeGrado, W. F. *J Biol Chem* 1987, 262, 6500–6505.
15. Wharton, S. A.; Martin, S. R.; Ruigrok, R. W. H.; Skehel, J. J.; Wiley, D. C. *J Gen Virol* 1988, 69, 1847–1857.
16. Rafalski, M.; Ortiz, A.; Rockwell, A.; van Ginkel, L. C.; Lear, J. D.; DeGrado, W. F.; Wilschut, J. *Biochemistry* 1991, 30, 10211–10220.
17. Gray, C.; Tatulian, S. A.; Wharton, S. A.; Tamm, L. K. *Biophys J* 1996, 70, 2275–2286.
18. Han, X.; Steinhauer, D. A.; Wharton, S. A.; Tamm, L. K. *Biochemistry*, 1999, 38, 15052–15059.
19. Tamm, L. K.; Tatulian, S. A. *Q Rev Biophys* 1997, 34, 365–429.
20. Ishiguro, R.; Kimura, M.; Takahashi, S. *Biochemistry* 1993, 32, 9792–9797.
21. Lüneberg, J.; Martin, I.; Nüssler, F.; Ruyschaert, J.-M.; Herrmann, A. *J Biol Chem* 1995, 270, 27606–27614.
22. Epand, R. M.; Epand, R. F.; Martin, I.; Ruyschaert, J.-M. *Biochemistry* 2001, 40, 8800–8807.
23. Han, X.; Tamm, L. K. *J Mol Biol* 2000, 304, 953–965.

24. Han, X.; Bushweller, J. H.; Cafiso, D. S.; Tamm, L. K. *Nature Struct Biol* 2001, 8, 715–720.
25. Altenbach, C.; Greenhalgh, D. A.; Khorana, H. G.; Hubbell, W. L. *Proc Natl Acad Sci USA* 1994, 91, 1667–1671.
26. Epand, R. M.; Epand, R. F. *Biochem Biophys Res Comm* 1994, 202, 1420–1425.
27. Melikyan, G. B.; Brener, S. A.; Ok, D. C.; Cohen, F. S. *J Cell Biol* 1997, 136, 995–1005.
28. Chernomordik, L. V.; Frolov, V. A.; Leikina, E.; Bronk, P.; Zimmerberg, J. J. *Cell Biol* 1998, 140, 1369–1382.
29. Lis, L. J.; McAlister, M.; Fuller, N.; Rand, R. P.; Parsegian, V. A. *Biophys J* 1982, 37, 657–665.
30. Tatulian, S. A.; Hinterdorfer, P.; Baber, G.; Tamm, L. K. *EMBO J* 1995, 14, 5514–5523.
31. Gray, C.; Tamm, L. K. *Protein Sci* 1998, 7, 2359–2373.
32. Tatulian, S. A.; Tamm, L. K. *Biochemistry* 2000, 39, 496–507.
33. Armstrong, R. T.; Kushnir, A. S.; White, J. M. *J Cell Biol* 2000, 151, 425–437.
34. MacKenzie, K. R.; Prestegard, J. H.; Engelman, D. M. *Science* 1997, 276, 131–133.